Letter

Skyrme force for all known Ξ^- hypernuclei

Jing Guo (郭静) and Xian-Rong Zhou (周先荣)*
Department of Physics, East China Normal University, Shanghai 200241, China

H.-J. Schulze
INFN Sezione di Catania, Dipartimento di Fisica, Universitá di Catania, Via Santa Sofia 64, I-95123 Catania, Italy

(Received 27 July 2021; revised 26 October 2021; accepted 9 December 2021; published 22 December 2021)

Recent experimental results for the cascade hypernucleus ${}^{15}_{\Xi}$C (^{14}N + Ξ^-) are analyzed together with data for ${}^{12}_{\Xi}$Be and ${}^{13}_{\Xi}$B within a Skyrme-Hartree-Fock theoretical approach. Optimal Skyrme parameters are determined for a consistent description of the KISO, IBUKI, KINKA, BNL-E885, BNL-E906, KEK-E224, and KEK-E176 data regarding these nuclei. The important role of deformation for ${}^{13}_{\Xi}$B is pointed out. The shape of the Ξ^- mean field in ${}^{12}_{\Xi}$Be is analyzed in some detail.

DOI: 10.1103/PhysRevC.104.L061307

Introduction. The experimental and theoretical study of hypernuclei is important because it allows access to the strangeness sector of the strong interaction and related physical phenomena at high energies and densities, in particular in astrophysics [1–3].

While Λ hypernuclei have been amply studied for several decades and the properties of the Λ-nucleon interaction are reasonably well known [4–6], the situation for the heavier Σ and Ξ hyperons is much more difficult and only a few hypernuclear data are available that are furthermore often burdened by ambiguities in their identification and interpretation [7–9]. Recently, however, new data on Ξ^- hypernuclei have become available at the J-PARC and KEK experimental facilities [10]. This work is an attempt to analyze all current data within the Skyrme-Hartree-Fock (SHF) theoretical approach and to determine an optimal set of ΞN interaction parameters capable of describing consistently most data.

We first briefly review the available data for the Ξ hypernuclei ${}^{15}_{\Xi}$C (^{14}N + Ξ^-), ${}^{13}_{\Xi}$B (^{12}C + Ξ^-), and ${}^{12}_{\Xi}$Be (^{11}B + Ξ^-). Most of them are nuclear emulsion events occurring after a $K^- p \to K^+ \Xi^-$ reaction. The most recent results regard ${}^{15}_{\Xi}$C. Analysis of the KEK-E373-T2 (KISO) event [9,11] provided the first clear evidence that this is a (Coulomb-assisted) strongly bound hypernucleus, produced in the reaction Ξ^- + ^{14}N $\to$ ${}^{15}_{\Xi}$C $\to$ ${}^{10}_{\Lambda}$Be + ${}^{5}_{\Lambda}$He. It is interpreted [9,12,13] as production of a Ξ^- $1p$ state with a removal energy $B_\Xi = 1.03 \pm 0.18$ MeV, leaving ${}^{10}_{\Lambda}$Be in an excited state after its decay. More recently, the J-PARC-E07-T006 (IBUKI) event [14] confirmed this result with $B_\Xi = 1.27 \pm 0.21$ MeV, and also KEK-E176 #14-03-35 indicates a possible compatible value, $B_\Xi = 1.18 \pm 0.22$ MeV [15]. The combined analysis of KISO and IBUKI yields $B_\Xi = 1.13 \pm 0.14$ MeV [14].

Recently higher B_Ξ values have been extracted for some events and are interpreted as possible Ξ^- $1s$ bound states [13]. These are the J-PARC-E07-T010 (IRRAWADDY), $B_\Xi = 6.27 \pm 0.27$ MeV, and the KEK-E373-T3 (KINKA), $B_\Xi = 8.00 \pm 0.77$ MeV or $B_\Xi = 4.96 \pm 0.77$ MeV, events. None of these are uniquely identified and therefore only one or none of these values may be realistic. In fact their error bars are nonoverlapping. We therefore consider in the following only one of these values as realistic and examine the consistency with the other data. This is the KINKA (8.00 MeV) result. We verified that the lower values produce a very inferior global description of the complete data set, as discussed in detail later.

Regarding the ${}^{12}_{\Xi}$Be hypernucleus, in the BNL-E885 counter experiment [16] the cross section for Ξ^- production in the threshold region of the ^{12}C(K^-, K^+) ${}^{12}_{\Xi}$Be reaction was interpreted by assuming a Ξ^--nucleus Woods-Saxon (WS) potential with a depth of about 14 MeV. In contrast with the individual emulsion events, this analysis was based on $\approx 3 \times 10^5$ scattering events. The result is consistent with the estimate $V_{\text{WS}} < 20$ MeV of the preceding KEK-E224 [17], and $V_{\text{WS}} = 17 \pm 6$ MeV in ${}^{9}_{\Xi}$He (^{8}Li + Ξ^-) of BNL-E906 [18], while the sequel J-PARC-E05 experiment on ${}^{12}_{\Xi}$Be remained so far inconclusive, reporting a preliminary possible one-peak interpretation with $B_\Xi \approx 6.3$ MeV or a two-peak interpretation with $B_\Xi \approx 9$ and 2 MeV [19].

Finally, there are several older KEK-E176 emulsion data [15,20] that can be understood as possible formations of ${}^{13}_{\Xi}$B. However, for none of those is a unique interpretation given. In particular, the events KEK-E176 #10-9-6, $B_\Xi = 0.82 \pm 0.17$ MeV, and KEK-E176 #13-11-14, $B_\Xi = 0.82 \pm 0.14$ MeV, might both be interpreted as ${}^{13}_{\Xi}$B$(1p)$ states [20–22], and this will also be included in our analysis.

These are the data that we confront with the theoretical SHF model in the following. This work is organized as follows: First the theoretical method and interaction are briefly described. Then the numerical results and corresponding discussions for ${}^{15}_{\Xi}$C, ${}^{13}_{\Xi}$B, and ${}^{12}_{\Xi}$Be are presented, and a summary is given.

*xrzhou@phy.ecnu.edu.cn

Formalism. The SHF mean-field method is a powerful theoretical density-functional approach which can be globally applied from light to heavy (hyper)nuclei [23,24]. In particular, this approach has also been employed successfully for light Λ hypernuclei with $A \approx 10$ [25–28] and a global ΛN Skyrme force SLL4 has been devised that fits very accurately the complete data set of currently known Λ hypernuclei [27,28].

In the present work, we study Ξ hypernuclei with $A = 12$, 13, and 15 and focus on the Ξ^- $1s$ and $1p$ states and their hyperon separation energy,

$$B_\Xi \equiv E([n,p,-]) - E([n,p,\Xi^-]) = E[^{A-1}(Z+1)] - E[^{A}_{\Xi}Z]. \quad (1)$$

Thus, as long as the rearrangement of the nuclear core $[n, p]$ by the added hyperon is not very large, for this observable one can expect that a major part of an inaccurate description of the common nuclear core cancels out, and that other uncertainties regarding the core such as center-of-mass (c.m.), pairing, deformation corrections, etc. become much less relevant. The removal energy then depends predominantly on the phenomenological ΞN interaction parameters that we adjust to the data, i.e., the hyperon-nucleus mean field. Therefore, it is expected that we can make robust theoretical predictions for the removal energies of these hypernuclei. As a further consequence, the hyperon removal energy is nearly independent of the specific (realistic) NN interaction that is used in the calculation [29].

It should also be noted that the Ξ^- hypernuclei decay into double-Λ hypernuclei by the ΞN-$\Lambda\Lambda$ coupling [30]. Therefore, the ΞN interaction should have an imaginary part to represent the decay width. However, since we have so far no useful experimental information on this coupling by Refs. [11,13–17], here the imaginary part is omitted.

We employ a model based on the self-consistent SHF method [23,24], first extended to the theoretical description of Λ hypernuclei in Ref. [25], and now used for hyperons $Y = \Xi^-$ here. The fundamental SHF local energy-density functional of hypernuclear matter is written as

$$\varepsilon_{\rm SHF} = \varepsilon_N + \varepsilon_Y, \quad (2)$$

and depends on the one-body densities ρ_q, kinetic densities τ_q, and spin-orbit currents $\boldsymbol{J}_q$,

$$[\rho_q,\ \tau_q,\ \boldsymbol{J}_q] = \sum_{i=1}^{N_q} n_q^i \Big[|\phi_q^i|^2,\ |\nabla\phi_q^i|^2,\ \phi_q^{i*}(\nabla\phi_q^i \times \boldsymbol{\sigma})/i \Big], \quad (3)$$

where ϕ_q^i $(i = 1, N_q)$ are the self-consistently calculated single-particle (s.p.) wave functions of the N_q occupied states for the species $q = n, p, Y$ in a hypernucleus.

The functional ε_N is the usual nucleonic part [23,24] and a possible standard parametrization for the hyperonic part is [12,21,25,27,28]

$$\varepsilon_Y = \frac{\tau_Y}{2m_Y} + a_0\rho_Y\rho_N + a_3\rho_Y\rho_N^\alpha + a_1(\rho_Y\tau_N + \rho_N\tau_Y) - a_2(\rho_Y\Delta\rho_N + \rho_N\Delta\rho_Y)/2 - a_4(\rho_Y\nabla\cdot\boldsymbol{J}_N + \rho_N\nabla\cdot\boldsymbol{J}_Y), \quad (4)$$

from which one obtains the corresponding hyperonic SHF mean fields

$$V_Y = a_0\rho_N + a_1\tau_N - a_2\Delta\rho_N - a_4\nabla\cdot\boldsymbol{J}_N + a_3\rho_N^\alpha, \quad (5)$$

$$V_N^{(Y)} = a_0\rho_Y + a_1\tau_Y - a_2\Delta\rho_Y - a_4\nabla\cdot\boldsymbol{J}_Y + a_3\alpha\rho_Y\rho_N^{\alpha-1}, \quad (6)$$

and a hyperon effective mass

$$\frac{1}{2m_Y^*} = \frac{1}{2m_Y} + a_1\rho_N. \quad (7)$$

The relation to the equivalent YN Skyrme-force parameters $t_{0,1,2,3}^{YN}$ [25] is

$$a_0 = t_0, \quad a_1 = \frac{t_1 + t_2}{4}, \quad a_2 = \frac{3t_1 - t_2}{8}, \quad a_3 = \frac{3t_3}{8}. \quad (8)$$

The "three-body" parameter α is kept here at its standard value of two, but also an alternative value of $7/6$, used in several NN Skyrme forces, is evaluated.

Minimizing the total energy of the hypernucleus, $E = \int d^3\boldsymbol{r}\,\varepsilon_{\rm SHF}(\boldsymbol{r})$, one arrives at the SHF Schrödinger equation

$$\left[\nabla\cdot\frac{1}{2m_q^*(\boldsymbol{r})}\nabla - V_q(\boldsymbol{r}) - e_qV_C(\boldsymbol{r}) + i\boldsymbol{W}_q(\boldsymbol{r})\cdot(\nabla\times\boldsymbol{\sigma})\right]\phi_q^i(\boldsymbol{r}) = e_q^i\phi_q^i(\boldsymbol{r}), \quad (9)$$

where V_C is the Coulomb field and $\boldsymbol{W}_N$ the nucleonic spin-orbit mean field [24]. In contrast to Λ hypernuclei, the Coulomb interaction is very important for the light Ξ^- hypernuclei discussed here and provides a substantial part of the Ξ^- binding. An approximate c.m. correction is applied as usual [23,24,31] by replacing the bare masses:

$$\frac{1}{m_q} \to \frac{1}{m_q} - \frac{1}{M}, \quad (10)$$

where $M = (N_n + N_p)m_N + N_Y m_Y$ is the total mass of the (hyper)nucleus. Solving the Schrödinger equation provides the wave functions $\phi_q^i(\boldsymbol{r})$ and the s.p. energies $-e_q^i$ for the different s.p. levels i and species q. We use in this work the standard nucleonic Skyrme force SLy4 [32], but the results for hyperonic observables hardly depend on that choice [29].

While the core nuclei ^{14}N and ^{11}B are (nearly) spherical, ^{12}C is an axially deformed oblate nucleus [21,33–38], and this will be very important for the data analysis later. Therefore, in this case a 2D SHF calculation is required. In our approach, we assume axial symmetry of the mean field, and the deformed SHF Schrödinger equation is solved in cylindrical coordinates (r, z) within the axially deformed harmonic-oscillator basis [23,24]. The geometric quadrupole deformation parameter of the nuclear core is expressed as

$$\beta_2 \equiv \sqrt{\frac{\pi}{5}}\frac{\langle 2z^2 - r^2\rangle}{\langle r^2 + z^2\rangle}. \quad (11)$$

We now discuss the choice of the five ΞN interaction parameters a_i. There are currently not enough data to determine uniquely all of them. We therefore proceed as follows: The effective-mass parameter a_1 is kept zero, motivated by the fact that recent Brueckner-Hartree-Fock calculations [39] indicate that the Ξ^- s.p. spectrum is rather flat and thus m_Ξ^*/m_Ξ is close to unity. Also, the spin-orbit parameter is disregarded,

TABLE I. The removal energies B_Ξ (in MeV) for the Ξ^- $1s$ and $1p$ states of $^{13}_{\Xi}$B and $^{12}_{\Xi}$Be, obtained with ΞN Skyrme forces of different parameters α and a_0 [MeV fm^3], a_2 [MeV fm^5], and a_3 [MeV fm$^{3\alpha}$] ($a_1 = a_4 = 0$). With these parameters, the Ξ^- $1s$ and $1p$ removal energies of $^{15}_{\Xi}$C are fixed to 8.00 and 1.13 MeV, respectively. $^{13}_{\Xi}$B values in brackets are for spherical calculations.

α	a_2	a_0	a_3	$^{13}_{\Xi s}$B	$^{13}_{\Xi p}$B	$^{12}_{\Xi s}$Be
	0	−200.3	704.8	6.62 (6.71)	0.86 (−0.12)	5.83
	10	−198.7	641.3	6.49 (6.65)	0.75 (−0.11)	5.72
2	20	−196.9	576.8	6.37 (6.59)	0.65 (−0.09)	5.61
	30	−194.7	509.3	6.25 (6.53)	0.56 (−0.08)	5.51
	40	−192.5	443.0	6.14 (6.46)	0.47 (−0.07)	5.40
	0	−498.6	551.3	6.44 (6.84)	0.84 (−0.07)	5.87
	10	−470.8	503.0	6.32 (6.76)	0.73 (−0.06)	5.76
7/6	20	−439.4	449.3	6.21 (6.69)	0.63 (−0.06)	5.64
	30	−409.0	397.3	6.10 (6.61)	0.54 (−0.05)	5.53
	40	−378.9	345.5	6.02 (6.54)	0.47 (−0.04)	5.42

$a_4 = 0$, as an inclusion of Ξ^- spin-orbit splitting is clearly premature. For the same reason we do not introduce further parameters for the isospin dependence of the interaction, e.g., $a_0\rho_N \to a_0^n\rho_n + a_0^p\rho_p$, at this stage.

The surface-energy parameter a_2 has no directly observable effect but is essential to determine the *shape* of the Ξ^- mean field V_Ξ in the hypernucleus, Eq. (5), which is important for comparison with the WS mean field that was used in the experimental analysis of $^{12}_{\Xi}$Be [16]. Motivated by the equivalent parameter value ($a_2^{N\Lambda} \approx 20$ MeV fm^5) of the recently derived SLL4 ΛN Skyrme force [28], we use several trial values of this parameter, $a_2 = 0, 10, \ldots, 40$ MeV fm^5.

For fixed $a_1 = a_4 = 0$ and the chosen a_2, the remaining and most important volume parameters a_0 and a_3 are then determined by fitting the removal energies $B_\Xi = 8.00$ and 1.13 MeV for the Ξ^- $1s$ and $1p$ states in $^{15}_{\Xi}$C, respectively, as claimed for the KINKA and KISO + IBUKI events. The Ξ^- mean field V_Ξ of the resulting solutions can then be compared with the WS mean field in $^{12}_{\Xi}$Be,

$$V_{\mathrm{WS}}(r) = \frac{-V_0}{1+\exp\left[(r-2.52\ \mathrm{fm})/0.65\ \mathrm{fm}\right]}, \qquad (12)$$

with $V_0 = 12$, 14, 16, 18, 20 MeV used in the analysis of BNL-E885, Refs. [11,16], and $V_0 \approx 14$ MeV identified as the preferred value. We now present the results of this procedure.

Results and discussion. Table I lists the parameter values a_0, a_2, and a_3 obtained following the above procedure, together with the Ξ^- $1s$ and $1p$ removal energies of $^{13}_{\Xi}$B and $^{12}_{\Xi}$Be that are predicted. Strongly bound $1p$ states with positive removal energies are only found for deformed $^{13}_{\Xi}$B nuclei, but not in spherical approximation (numbers in brackets).

In general one obtains reasonable values for the parameters a_0 and a_3, in particular for the parameter a_3 that can be related to the nonlinear density dependence of the Ξ^- mean field in homogeneous nuclear matter,

$$V_\Xi(\rho_N) = a_0\rho_N + a_1\tau_N + a_3\rho_N^\alpha. \qquad (13)$$

For comparison, in the SLL4 ΛN Skyrme force [27,28], the equivalent optimal parameter is $a_3^{\Lambda N} \approx 700$ MeV fm^6, whereas $a_3^{NN} \approx O(2000$ MeV fm$^6)$ in typical nucleonic Skyrme forces [24]. For increasing surface parameter a_2, an increasing part of the Ξ^- binding is provided by the associated terms in Eqs. (4) and (5), and therefore both a_0 and a_3 decrease in magnitude.

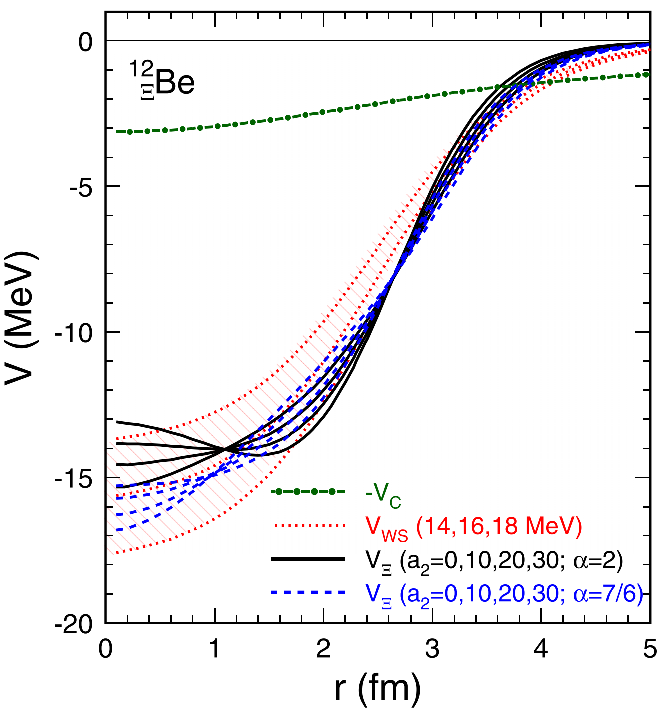

FIG. 1. Local Ξ^- mean field V_Ξ and Coulomb field $-V_C$ in $^{12}_{\Xi}$Be obtained with the SHF models with various forces in Table I. Increasing values of a_2 produce deeper well depths $V_\Xi(0)$. The Woods-Saxon mean field deduced in Ref. [16] is shown for comparison.

To interpret the different results we now discuss the associated potentials V_Ξ. In Fig. 1, the different SHF mean-field potentials in the $^{12}_{\Xi}$Be hypernucleus are plotted, including the local Coulomb field V_C, the strong mean field V_Ξ, Eq. (5), and for comparison the WS mean field (12) with $V_0 = 14$, 16, 18 MeV, as used in the analysis of BNL-E885 [11,16]. One observes that the SHF results cover the range between the 14 and 18 MeV curves, with $V_\Xi(0) \approx 15$ MeV. We consider this as a very good agreement with the analysis of E885. In fact, in that analysis the quasiparticle peak of $^{12}_{\Xi s}$Be for $V_0 = 14$ MeV is located at about 5 MeV [16], although spread out by the experimental resolution (see also Refs. [8,12,20,40,41]), close to our results in Table I. It can clearly be seen in the figure that the zero-momentum value $V_\Xi(0)$ alone is obviously not a useful unique indicator of the interaction strength, as the shape of the mean field controlled by the parameter a_2 plays an essential role. A value of about $a_2 \approx 20$–30 MeV fm^5 gives the closest correspondence to a WS shape, whereas $a_2 = 0$ generates a flat or nonmonotonic shape in the core region. Values of $V_\Xi(0)$ obtained in theoretical approaches different from a WS description have therefore to be interpreted with great care in confrontation with E885.

The hypernuclei $^{15}_{\Xi}$C and $^{12}_{\Xi}$Be and their core nuclei discussed so far are spherical nuclei. The case of $^{13}_{\Xi}$B is more delicate, as the core nucleus ^{12}C is axially deformed in the SHF approach [21,33–38]. As discussed in detail in Ref. [21], its oblate deformation favors the binding of a Ξ^- 1p orbital because of the improved geometrical overlap of wave function and embedding potential, such that this state becomes more bound than in spherical approximation.

The deformation of the core nucleus ^{12}C derived from its proton quadrupole moment Q_p is rather large [42],

$$\beta \equiv \frac{\sqrt{5\pi}}{3}\frac{Q_p}{ZR_0^2} \approx -0.58 \pm 0.03, \tag{14}$$

with $R_0 \equiv 1.2A^{1/3}$ fm. In the SHF approach the size of nuclear deformation can be controlled by adjusting the spin-orbit parameter of the NN Skyrme force [21,33–38], and we follow this procedure to reproduce the proper β value and to estimate quantitatively the effect on the embedded Ξ^-. The results of Table I for $^{13}_{\Xi}$B are obtained in this way and demonstrate that the proposed interpretation of the KEK-E176 events as $^{13}_{\Xi p}$B states might be purely due to the fact that ^{12}C is a strongly deformed nucleus. Excellent agreement with the experimental value $B_\Xi \approx 0.82$ MeV is obtained with small values of a_2 and both choices of α. Thus, in principal, the proper a_2 value could be determined by fitting $B_\Xi = 0.82$ MeV, but with the current state of the art it seems premature to draw a quantitative conclusion here.

To illustrate the mechanism that lowers the p-state energies in the deformed core nucleus, we plot in Fig. 2 the total Ξ^- mean field $V_\Xi - V_C$ (upper panel) and the density distribution ρ_Ξ (lower panel) in the deformed nucleus $^{13}_{\Xi p}$B for the parameter set with $\alpha = 2$ and $a_2 = 0$ in Table I. The results for $z = 0$ (solid curves) and $r = 0$ (dashed curve) are shown, in comparison with those of the spherical calculation (dotted curves). One sees clearly that for the oblately deformed nucleus the potential well in the $z = 0$ plane is deeper by several MeV in the region around $r \approx 3$ fm, where a major part of the oblate Ξ^- 1p [101] wave function resides. This leads to an energy gain of the order of 1 MeV for the binding of the Ξ^-.

One also notes that the density of the Ξ^- 1p states is well concentrated inside the core nucleus and they are therefore states bound by the ΞN strong interaction, assisted by the Coulomb attraction. This is in contrast with the infinite set of weakly bound atomic Coulomb states 2P, 3D, ... located far outside the nuclear core with s.p. energies of about 0.3, 0.1, ... MeV [9,22], which are not addressed in this work. Their properties have been amply studied in the past [43–47], but their modification by the nuclear core is practically negligible.

Finally, we remark that the alternative and mutually exclusive interpretations of the KEK-E176 #13-11-14 event [11,15,20] with $B_\Xi = 2.84 \pm 0.25$ MeV or $B_\Xi = 3.89 \pm 0.14$ MeV are excluded by our combined analysis as either $^{13}_{\Xi s}$B or $^{13}_{\Xi p}$B states, since they would be incompatible with both the $^{15}_{\Xi}$C and $^{12}_{\Xi}$Be data.

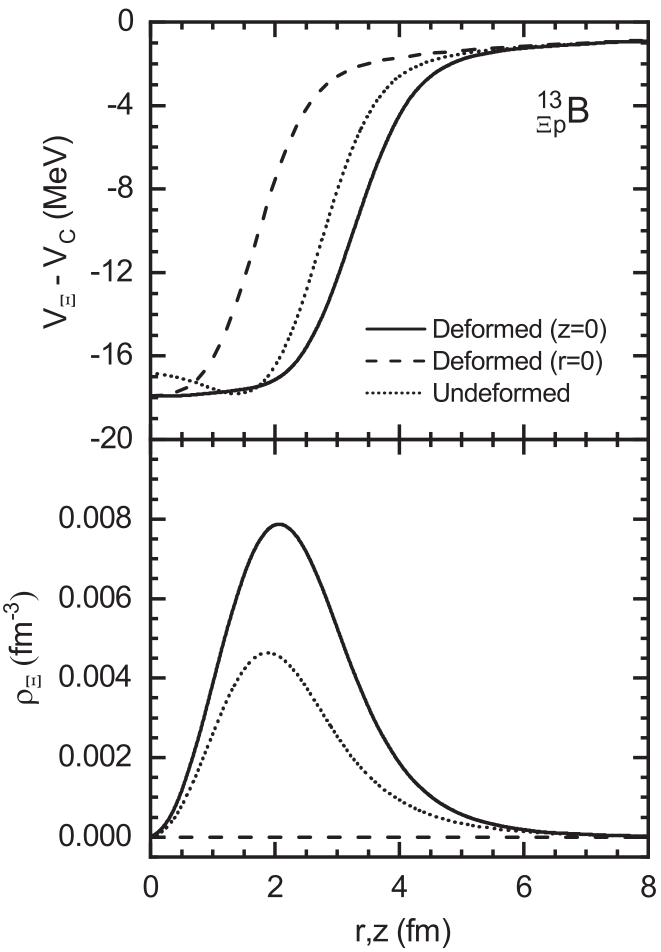

FIG. 2. Total Ξ^- mean field $V_\Xi - V_C$ (upper panel) and density distribution ρ_Ξ (lower panel) in the deformed nucleus $^{13}_{\Xi p}$B, obtained with the SHF model with $\alpha = 2$ and $a_2 = 0$ in Table I. The results for $z = 0$ (solid curves) and $r = 0$ (dashed curves) are shown. The dotted curves show the result for the spherical calculation.

Summary. We have tried to fit all current data for the cascade hypernuclei $^{15}_{\Xi}$C, $^{12}_{\Xi}$Be, and $^{13}_{\Xi}$B within a global SHF approach for the ΞN interaction. Our main conclusions are as follows:

(1) Of all proposed $B_\Xi(^{15}_{\Xi s}\text{C})$ values, the KINKA (8.00 MeV) interpretation seems to be the one most compatible with both the $^{12}_{\Xi}$Be and $^{13}_{\Xi}$B data, although slightly lower values down to about 7 MeV might also be possible and consistent with $^{12}_{\Xi}$Be, but would not allow interpretation of the KEK-176 events as $^{13}_{\Xi p}$B states. This means that both the IRRAWADDY (6.27 MeV) and the KINKA (4.96 MeV) interpretation of $^{15}_{\Xi s}$C clash with the $^{12}_{\Xi}$Be and $^{13}_{\Xi}$B data.

(2) Combining KINKA ($^{15}_{\Xi s}$C) and KISO + IBUKI ($^{15}_{\Xi p}$C) data, the predicted Ξ^- mean field in $^{12}_{\Xi}$Be is very similar to the best-choice WS mean field for BNL-E885 of Ref. [16] with a depth of about 14–16 MeV, and also compatible with KEK-E224 [17] and BNL-E906 [18]. Also the preliminary one-peak interpretation of

the J-PARC-E05 experiment [19] would be in good agreement with this result. The limited resolution of BNL-E885, the large error bar of KINKA (8.00 ± 0.77 MeV), and the dependence on the a_2 parameter mean that only a qualitative conclusion can be drawn here at this time.

(3) ${}^{13}_{\Xi}$B is a delicate case, as in the current model this hypernucleus and its core nucleus ^{12}C are strongly axially deformed, and the claimed $B_\Xi \approx 0.8$ MeV values of some KEK-E176 emulsion data might be explained as a consequence of this deformation, which energetically favors the extended Ξ^- $1p$ orbit. Again the global Skyrme force would be quantitatively compatible with this interpretation. Treating these nuclei as undeformed will not produce a sufficiently bound Ξ^- $1p$ state (which is in fact another possible interpretation of the data).

The proposed Skyrme force SLX3 with moderate values of the parameter a_2 is thus able to fit satisfactorily all current data, although due to the limited accuracies and the ambiguities of the data a firm statement cannot yet be made. This situation is expected to improve soon because a large number of emulsion events obtained in KEK-E373 and J-PARC-E07 still await their analysis. Our prediction will be confronted with these future data, which will also serve to constrain better the SHF ΞN interaction parameters, including the less-important parameters a_1 and α and the isospin dependence of the interaction. Further improvements of the approach would also include going beyond the mean-field treatment and including the imaginary parts due to the ΞN-$\Lambda\Lambda$ decay.

Acknowledgments. This work was supported by the National Natural Science Foundation of China under Contracts No. 11775081 and No. 12175071, and the Natural Science Foundation of Shanghai under Contract No. 17ZR1408900.

[1] J. Schaffner-Bielich, Nucl. Phys. A **804**, 309 (2008); **835**, 279 (2010).

[2] M. Oertel, M. Hempel, T. Klähn, and S. Typel, Rev. Mod. Phys. **89**, 015007 (2017).

[3] G. F. Burgio, H.-J. Schulze, I. Vidaña, and J.-B. Wei, Prog. Part. Nucl. Phys. **120**, 103879 (2021).

[4] O. Hashimoto and H. Tamura, Prog. Part. Nucl. Phys. **57**, 564 (2006).

[5] A. Feliciello and T. Nagae, Rep. Prog. Phys. **78**, 096301 (2015).

[6] A. Gal, E. V. Hungerford, and D. J. Millener, Rev. Mod. Phys. **88**, 035004 (2016).

[7] B. Dover and A. Gal, Ann. Phys. (NY) **146**, 309 (1983).

[8] Y. Yamamoto, T. Motoba, T. Fukuda, M. Takahashi, and K. Ikeda, Prog. Theor. Phys. Suppl. **117**, 281 (1994).

[9] E. Hiyama and K. Nakazawa, Annu. Rev. Nucl. Part. Sci. **68**, 131 (2018).

[10] H. Ohnishi, F. Sakuma, and T. Takahashi, Prog. Part. Nucl. Phys. **113**, 103773 (2020).

[11] K. Nakazawa *et al.*, Prog. Theor. Exp. Phys. **2015**, 033D02 (2015).

[12] T. T. Sun, E. Hiyama, H. Sagawa, H.-J. Schulze, and J. Meng, Phys. Rev. C **94**, 064319 (2016).

[13] M. Yoshimoto *et al.*, Prog. Theor. Exp. Phys. **2021**, 073D02 (2021).

[14] S. H. Hayakawa *et al.* (J-PARC E07 Collaboration), Phys. Rev. Lett. **126**, 062501 (2021).

[15] S. Aoki *et al.* (KEK E176 Collaboration), Prog. Theor. Phys. **89**, 493 (1993); Phys. Lett. B **355**, 45 (1995); Nucl. Phys. A **828**, 191 (2009).

[16] P. Khaustov, D. E. Alburger, P. D. Barnes, B. Bassalleck, A. R. Berdoz, A. Biglan, T. Burger, D. S. Carman, R. E. Chrien, C. A. Davis, H. Fischer, G. B. Franklin, J. Franz, L. Gan, A. Ichikawa, T. Iijima, K. Imai, Y. Kondo, P. Koran, M. Landry *et al.* (AGS E885 Collaboration), Phys. Rev. C **61**, 054603 (2000).

[17] T. Fukuda, A. Higashi, Y. Matsuyama, C. Nagoshi, J. Nakano, M. Sekimoto, P. Tlusty, J. K. Ahn, H. Enyo, H. Funahashi, Y. Goto, M. Iinuma, K. Imai, Y. Itow, S. Makino, A. Masaike, Y. Matsuda, S. Mihara, N. Saito, R. Susukita *et al.* (E224 Collaboration), Phys. Rev. C **58**, 1306 (1998).

[18] T. Tamagawa *et al.* (BNL-E906 Collaboration), Nucl. Phys. A **691**, 234 (2001); T. Harada and Y. Hirabayashi, Phys. Rev. C **103**, 024605 (2021).

[19] T. Nagae *et al.* (J-PARC E05 collaboration), AIP Conf. Proc. **2130**, 020015 (2019).

[20] Y. Yamamoto and T. Motoba, Nucl. Phys. A **585**, 371 (1995); Y. Yamamoto, in *Mesons and Light Nuclei '95*, Few-Body Systems, Vol. 9, edited by J. Adam, J. Dobeš, R. Mach, M. Sotona, and J. Dolejší (Springer, Vienna, 1995); M. Yamaguchi, K. Tominaga, Y. Yamamoto, and T. Ueda, Prog. Theor. Phys. **105**, 627 (2001).

[21] Y. Jin, X.-R. Zhou, Y.-Y. Cheng, and H.-J. Schulze, Eur. Phys. J. A **56**, 135 (2020).

[22] E. Friedman and A. Gal, Phys. Lett. B **820**, 136555 (2021).

[23] D. Vautherin and D. M. Brink, Phys. Rev. C **5**, 626 (1972); D. Vautherin, *ibid.* **7**, 296 (1973).

[24] M. Bender, P.-H. Heenen, and P.-G. Reinhard, Rev. Mod. Phys. **75**, 121 (2003); J. R. Stone and P.-G. Reinhard, Prog. Part. Nucl. Phys. **58**, 587 (2007); J. Erler, P. Klüpfel, and P.-G. Reinhard, J. Phys. G **38**, 033101 (2011).

[25] M. Rayet, Ann. Phys. (NY) **102**, 226 (1976); Nucl. Phys. A **367**, 381 (1981).

[26] D. J. Millener, C. B. Dover, and A. Gal, Phys. Rev. C **38**, 2700 (1988); Y. Yamamoto, H. Bandō, and J. Zofka, Prog. Theor. Phys. **80**, 757 (1988); **83**, 254 (1990); F. Fernández, T. López-Arias, and C. Prieto, Z. Phys. A **334**, 349 (1989); D. E. Lanskoy and Y. Yamamoto, Phys. Rev. C **55**, 2330 (1997); D. E. Lanskoy, *ibid.* **58**, 3351 (1998); J. Cugnon, A. Lejeune, and H.-J. Schulze, *ibid.* **62**, 064308 (2000); Y. Yamamoto, T. Motoba, and T. A. Rijken, Prog. Theor. Phys. Suppl. **185**, 72 (2010); N. Guleria, S. K. Dhiman, R. Shyam *et al.*, Nucl. Phys. A **886**, 71 (2012).

[27] H.-J. Schulze and E. Hiyama, Phys. Rev. C **90**, 047301 (2014).

[28] H.-J. Schulze, AIP Conf. Proc. **2130**, 020009 (2019).

[29] Y. Zhang, H. Sagawa, and E. Hiyama, Phys. Rev. C **103**, 034321 (2021).

[30] Y. Yamamoto, M. Wakai, T. Motoba, and T. Fukuda, Nucl. Phys. A **625**, 107 (1997).

[31] M. Bender, K. Rutz, P.-G. Reinhard, and J. A. Maruhn, Eur. Phys. J. A **7**, 467 (2000).

[32] E. Chabanat, P. Bonche, P. Haensel, J. Meyer, and R. Schaeffer, Nucl. Phys. A **627**, 710 (1997); **635**, 231 (1998); **643**, 441 (1998).

[33] T. Suzuki, H. Sagawa, and K. Hagino, Phys. Rev. C **68**, 014317 (2003).

[34] H. Sagawa, X.-R. Zhou, X.-Z. Zhang, and T. Suzuki, Phys. Rev. C **70**, 054316 (2004).

[35] H.-J. Schulze, M. Thi Win, K. Hagino, and H. Sagawa, Prog. Theor. Phys. **123**, 569 (2010).

[36] J.-W. Cui, X.-R. Zhou, and H.-J. Schulze, Phys. Rev. C **91**, 054306 (2015).

[37] J.-W. Cui, X.-R. Zhou, L.-X. Guo, and H.-J. Schulze, Phys. Rev. C **95**, 024323 (2017).

[38] J.-W. Cui and X.-R. Zhou, Prog. Theor. Exp. Phys. **2017**, 093D04 (2017).

[39] H.-J. Schulze and T. Rijken, Phys. Rev. C **88**, 024322 (2013); Th. A. Rijken and H.-J. Schulze, Eur. Phys. J. A **52**, 21 (2016).

[40] E. Hiyama, Y. Yamamoto, T. Motoba, Th. A. Rijken, and M. Kamimura, Phys. Rev. C **78**, 054316 (2008).

[41] H. Matsumiya, K. Tsubakihara, M. Kimura, A. Dote, and A. Ohnishi, Phys. Rev. C **83**, 024312 (2011).

[42] N. J. Stone, At. Data Nucl. Data Tables **90**, 75 (2005); IAEA Nuclear Data Services, Reference Input Parameter Library, http://www-nds.iaea.org/RIPL-2/.

[43] J. H. Koch, M. M. Sternheim, and J. F. Walker, Phys. Rev. Lett. **26**, 1465 (1971).

[44] C. J. Batty, Phys. Lett. B **87**, 324 (1979).

[45] A. Gal, E. Friedman, and C. J. Batty, Nucl. Phys. A **606**, 283 (1996).

[46] C. J. Batty, E. Friedman, and A. Gal, Phys. Rep. **287**, 385 (1997).

[47] D. Gotta, Prog. Part. Nucl. Phys. **52**, 133 (2004).